

Thermal properties of $\text{Lu}_5\text{Ir}_4\text{Si}_{10}$ near the charge-density-wave transition

Y.-K. Kuo

Department of Physics, National Dong-Hwa University, Hualien 974, Taiwan

C. S. Lue, F. H. Hsu, H. H. Li, and H. D. Yang*

Department of Physics, National Sun-Yat-Sen University, Kaohsiung 804, Taiwan

(Received 16 October 2000; revised manuscript received 10 April 2001; published 11 September 2001)

We report the investigations of specific heat, thermal conductivity, as well as thermoelectric power on the charge-density-wave (CDW) compound $\text{Lu}_5\text{Ir}_4\text{Si}_{10}$ as a function of temperature. All thermal measurements consistently exhibit anomalous features around the CDW transition temperature $T_o \sim 80$ K. Although the observations can be associated with the CDW formation, the measured anomalies are significantly large, in contrast to those in weak-coupled CDW materials. A quantitative analysis for the specific-heat data near the fluctuation region yields a critical exponent $\alpha \sim 2$, much larger than the predicted value $\alpha = 0.5$ in the extended mean-field theory assuming three-dimensional fluctuations. We also obtained a ratio $\gamma^*/\gamma = 8.4$, a factor of 6 larger than the BCS value 1.43 in the weak-coupling limit, indicating a strong coupling of this phase transition. Besides, the observed giant excess specific heat $\Delta C_p/C_p \sim 26\%$ and thermal conductivity $\Delta\kappa/\kappa \sim 15\%$ at T_o further support this strong-coupling scenario. These large enhancements in C_p and κ are attributed to the results of substantially thermal excitation and heat carried by the soft phonons at the transition. In addition, a rapid change in the sign of thermoelectric power at T_o was observed, which provides a better understanding of the evolution of electronic band structure of the system below and above the CDW formation.

DOI: 10.1103/PhysRevB.64.125124

PACS number(s): 71.45.Lr, 71.20.Lp, 75.40.-s

I. INTRODUCTION

The formation of charge-density waves (CDW) in $\text{Lu}_5\text{Ir}_4\text{Si}_{10}$ has been proposed with the observations of sharp anomalies in the electrical resistivity and magnetic susceptibility at the transition temperature $T_o \sim 80$ K.¹ High-pressure resistivity experiments showed that T_o successively decreases with applied pressure P , resulting in the complete suppression of this phase transition at a critical pressure $P_c = 21$ kbars.¹ The removal of this phase transition by pressure correlates to a sudden enhancement of the superconducting transition temperature T_c from 3.8 K at ambient pressure to 9 K at the critical pressure.² Such pressure effects imply that the CDW ground state and superconductivity in this material complete with each other for the density of states as each opens up an energy gap over a portion of the Fermi surface. Other studies, such as ¹⁷⁵Lu nuclear magnetic resonance,³ thermal expansion,⁴ and impurity effects on $(\text{Lu}_{1-x}\text{Sc}_x)\text{Ir}_4\text{Si}_{10}$ and $\text{Lu}_5(\text{Ir}_{1-x}\text{Rh}_x)_4\text{Si}_{10}$ (Ref. 5) all support this CDW scenario. Unlike the conventional CDW materials usually found among low-dimensional systems,⁶ $\text{Lu}_5\text{Ir}_4\text{Si}_{10}$ crystallizes in the three-dimensional (3D) tetragonal $\text{Sc}_5\text{Co}_4\text{Si}_{10}$ structure. As far as we know, only few 3D materials exhibit CDW behavior. For example, the spinel compound CuV_2S_4 is a 3D lattice claimed to form CDW ground state.⁷ Hence, a direct structural evidence to confirm the CDW formation in $\text{Lu}_5\text{Ir}_4\text{Si}_{10}$ is crucial. More recently, Becker *et al.*⁸ and Galli *et al.*⁹ have successfully grown single crystals of $\text{Lu}_5\text{Ir}_4\text{Si}_{10}$ and $\text{Er}_5\text{Ir}_4\text{Si}_{10}$, with which the CDW superlattices in the x-ray diffraction were indeed observed. It is noted that there is no direct transition-metal-transition-metal binding in the $\text{Sc}_5\text{Co}_4\text{Si}_{10}$ structure, while they are connected to each other through rare-earth or Si atoms. Therefore, the $\text{Sc}_5\text{Co}_4\text{Si}_{10}$ structure could be visual-

ized as one-dimensional chains accompanied by possible interchain interactions.^{8,9}

In fact, $\text{Lu}_5\text{Ir}_4\text{Si}_{10}$ has been considered a strong interchain coupled intermetallic, as evidenced by the discovery of a huge specific-heat jump ($\Delta C_p \sim 160$ J/mol K) associated with an entropy change $\Delta S = 0.5R$ (where R is the gas constant) at T_o .⁸ Furthermore, the observed CDW transition has been suggested to be first order due to the spike-shaped anomaly in C_p and have the sharpest cusp with $\Delta T_o/T_o \sim 1\%$ among any reported CDW systems.⁸ In contrast to many weak-coupled CDW materials such as NbSe_3 ,¹⁰ the thermodynamic properties of the strong-coupled systems usually require a description beyond the mean-field theory since the corresponding short coherence length would lead to significant phonon softening near the CDW transition, as proposed by McMillan.¹¹ To further explore the thermodynamic property of the transition in $\text{Lu}_5\text{Ir}_4\text{Si}_{10}$, a denser and smoother specific-heat measurement near T_o was performed and the measured data were analyzed in accordance with the critical-fluctuation model. In addition, we have also studied the temperature-dependent thermal conductivity (κ) and thermoelectric power (TEP) of $\text{Lu}_5\text{Ir}_4\text{Si}_{10}$ to shed light on its peculiar CDW transition.

II. EXPERIMENTAL DETAILS

The preparation and characterization of polycrystalline $\text{Lu}_5\text{Ir}_4\text{Si}_{10}$ have been described previously.^{1,2} Briefly, samples were prepared by arch-melting stoichiometric mixtures of high-purity elements in a Zr-gettered argon atmosphere. The resulting ingots were turned and remelted at least five times to promote homogeneity. Samples were then sealed in quartz ampoules with about 160 Torr of argon and annealed at 1250 °C for one day followed by three days at 1050 °C.

Relative specific heats were performed with a high-resolution ac calorimeter,¹² using chopped light as a heat source. Photoabsorbing PbS film were evaporated on samples, which were sanded to a thickness of about 0.2 mm to ensure “one-dimensional” heat flow. The averaged and oscillating temperatures (T_{ac}) of the sample were detected by an E-type thermocouple of 25 μm diameter, attached with small amount of GE varnish. The frequency dependence of T_{ac} was measured at various temperatures to determine the correct range of chopping frequencies. For appropriately chosen chopping frequency (typically 2–12 Hz), the magnitude of the temperature oscillation is inversely proportional to the total heat capacity (including sample and addendum). Three $\text{Lu}_5\text{Ir}_4\text{Si}_{10}$ specimens were examined to check experimental reproducibility.

The thermal conductivity and thermoelectric power were carried out simultaneously in a close-cycle refrigerator over temperatures from 10 to 300 K, using a direct heat-pulse technique. Samples were cut to a rectangular parallelepiped shape of typical size of $1.5 \times 1.5 \times 5.0 \text{ mm}^3$ with one end glued (with thermal epoxy) to a copper block as a heat sink. A calibrated chip resistor (100 Ω at room temperature with size of $1.0 \times 0.5 \times 0.3 \text{ mm}^3$) served as a heat source was glued to the other end. The temperature difference was measured by an E-Type differential thermocouple with junctions thermally attached to two well-separated positions along the sample. The temperature difference was controlled to be less than 1 K to minimize the heat radiation. During measurements the sample space is maintained in a good vacuum (better than 10^{-4} Torr). All experiments were performed on warming at a rate slower than 20 K/h. The reproducibility of κ and TEP measurements is better than 2%, while the absolute accuracy of κ is approximately 20%, mainly due to the uncertainty of sample dimensions.

It is worthwhile addressing that all measured temperature-dependent features are reproducible for samples from various batches, but the observed anomalies are somewhat different. The sample dependence in κ and TEP is presumably due to the anisotropic effect for the heat transport and we thus present results on the sample with sharpest anomaly at T_o .

III. RESULTS AND DISCUSSIONS

A. Heat capacity

The T -dependent specific heat of $\text{Lu}_5\text{Ir}_4\text{Si}_{10}$ is illustrated in Fig. 1. Notice that the ac technique does not give the absolute value of specific heat without detailed knowledge of the power absorbed from the light pulse. The absolute value of the specific heat above 130 K is determined by measuring a powder sample (~ 200 mg) using a differential scanning

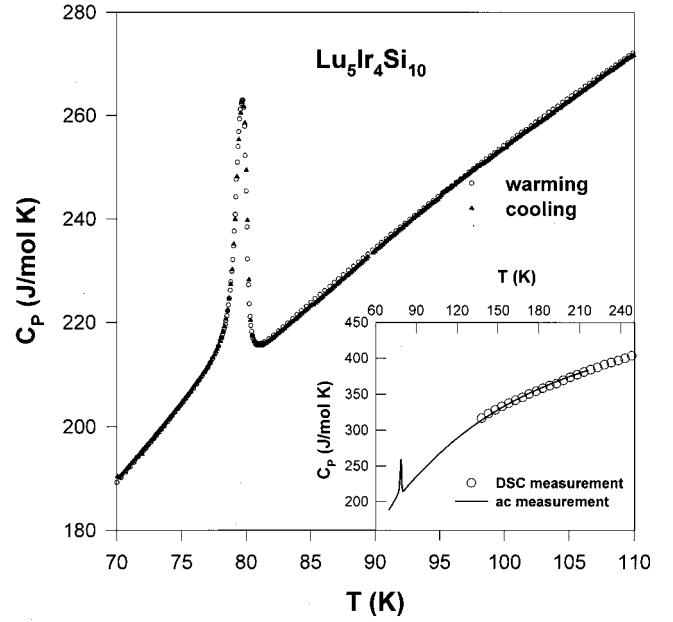


FIG. 1. The temperature dependence of specific heat measured on both warming and cooling for $\text{Lu}_5\text{Ir}_4\text{Si}_{10}$. No thermal hysteresis was observed within the resolution limit of our apparatus. The inset shows the matching between DSC and ac data.

calorimetry (DSC) with a precision better than 3%.¹³ The ac results were corrected for their addendum heat capacities (GE varnish and thermocouple wire) and normalized to the DSC data at 180 K. The differences between DSC and ac results are less than 2% at all matching temperatures, as shown in the inset of Fig. 1. The resulting temperature dependence and overall absolute values of specific heat are similar to those reported in Ref. 8. After subtracting a smooth background, estimated by fitting a lattice background through the data far from the transition, we obtain the specific heat jump $\Delta C_p = 55 \text{ J/mol K}$, entropy change $\Delta S = 0.12R$ and an excess specific heat $\Delta C_p/C_p \sim 26\%$ at the transition. These values are somewhat smaller than those obtained from single-crystal samples.⁸ The transition width ΔT_o , taking the temperature width of half-peak height, of about 1 K is close or even narrower than that presented by Becker and co-workers.⁸ A summary regarding the characteristics of the anomaly in $\text{Lu}_5\text{Ir}_4\text{Si}_{10}$ compared to that of the typical and well-studied CDW system $\text{K}_{0.3}\text{MoO}_3$ is listed in Table I. It is found that the anomaly of the former is much larger and sharper than that of the latter.

Although the CDW transition in $\text{Lu}_5\text{Ir}_4\text{Si}_{10}$ has been classified as first-order due to the spike-shaped anomaly in C_p ,⁸

TABLE I. Summary of specific-heat and thermal-conductivity anomalies of $\text{Lu}_5\text{Ir}_4\text{Si}_{10}$ compared to the well-studied CDW system $\text{K}_{0.3}\text{MoO}_3$.

	T_o (K)	$\Delta T_o/T_o$ (%)	ΔC_p (J/mol K)	ΔS (R)	$\Delta C_p/C_p$ (%)	$\Delta \kappa/\kappa$ (%)
$\text{Lu}_5\text{Ir}_4\text{Si}_{10}$	79.8	1	55	0.12	26	15
$\text{K}_{0.3}\text{MoO}_3^a$	180	11	8	0.18	6	5

^aData taken from Refs. 15, 17, and 18.

no thermal hysteresis near the phase transition is observed within the resolution limit of our apparatus (Our resistivity and magnetic susceptibility results also show no thermal hysteresis at T_o .) The specific-heat data in the vicinity of the transition was thus analyzed via a least-squares fitting procedure to a model of critical fluctuations in addition to BCS mean-field contributions from 65 to 100 K. In this respect, the specific heat C consist of three terms

$$C = C_L + C_{MF} + C_{fl} \quad (1)$$

where C_L is the lattice background, C_{MF} is the mean-field term below T_o , and C_{fl} is associated with fluctuation contributions. In this temperature range, we assume that the lattice specific heat has the form given from the Einstein model,

$$C_L = a_1 \left(\frac{a_2}{T} \right)^{a_3} \frac{e^{a_1/T}}{(e^{a_2/T} - 1)^2}. \quad (2)$$

In order to fit the total heat capacity, we need fitting functions expressed as

$$C^- = C_L + \gamma^* T_o (1 + \beta t) + b^- |t|^{-\alpha^-}, \quad T < T_o$$

$$C^+ = C_L + b^+ |t|^{-\alpha^+}, \quad T > T_o. \quad (3)$$

Here the mean-field term below T_o is represented by

$$C_{MF} = \gamma^* T_o (1 + \beta t), \quad (4)$$

and the fluctuation part is

$$C_{fl}^- = b^- |t|^{-\alpha^-}, \quad T < T_o$$

$$C_{fl}^+ = b^+ |t|^{-\alpha^+}, \quad T > T_o. \quad (5)$$

Here a_1 , a_2 , a_3 , γ^* , β , b^- , b^+ , α^- , and α^+ are effective fitting parameters, where α^- and α^+ are known as critical exponents and $t = (T_o - T)/T_o$ is the reduced temperature. Since the temperature range for fluctuations that is significant in our data is only about 5 K, a free least-squares fitting process would underestimate the importance of the critical piece. The fitting procedures were then taken as follows: we first set $T_o = 79.70$ K, and then used the specific-heat data above and away from T_o to find the best fitting values of a_1 , a_2 , and a_3 in C_L . With the obtained C_L , the optimum values of γ^* and β can be found by fitting the curve of specific heat below and near but not too close to T_o to the function of $C_L + C_{MF}$. We then determined the best-fitting values of b^- , α^- and b^+ , α^+ by adjusting the functions $(C_L + C_{MF} + C_{fl}^-)$ and $(C_L + C_{fl}^+)$ for temperatures below and above T_o , respectively, to match the measured specific-heat curve. The satisfactory agreement between the fit and measured data of Lu₅Ir₄Si₁₀ is shown in Fig. 2. These extracted fitting parameters, providing important information about the characteristics of transition, are listed in Table II. Representative values of critical exponents α^- and α^+ and their corresponding standard deviations are listed Table III. Notice that a logarithmic divergence ($C_{fl}^- = b^- \ln|t|$, $C_{fl}^+ = b^+ \ln|t|$) is also included in the table for comparison. The standard deviations of the fit are calculated with exclusion of the data points very

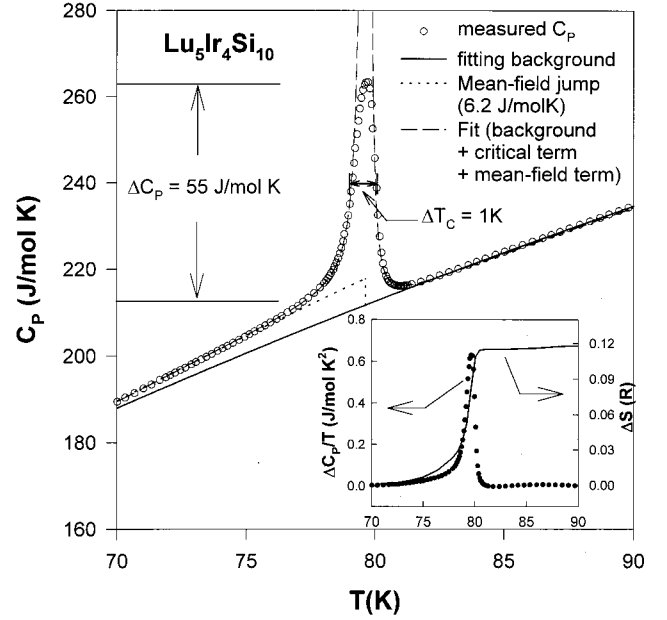


FIG. 2. The jump of specific heat ΔC_p and the agreement between the data points (open circles) and the fit points (broken curves) in the vicinity of CDW transition for Lu₅Ir₄Si₁₀. The inset shows the plots of $\Delta C_p/T$ vs T and entropy change ΔS associated with the transition.

near T_c ($T_c \pm 0.5$ K). These points would not follow a power law or logarithmic divergence due to the rounding effects by sample inhomogeneities. It turns out that the critical exponents α^- and α^+ extracted from the best fit are close to 2, much larger than the extended mean-field expectation of $\alpha^- = \alpha^+ = 0.5$ (poor fit to these data) normally seen in typical CDW materials.¹⁴⁻¹⁶ A higher power of divergence in C_p near T_o reflects the very narrow transition width, which in turn agrees with the fact that no pretransition fluctuations was observed by x-ray scattering experiments.⁸

Another important quantity $\gamma^* = 7.7 \times 10^{-2}$ J/mol K was also obtained from the fit. Here $\gamma^* T_o$ represents the electronic specific-heat jump of the mean-field term at the transition. From the magnetic-susceptibility measurement,¹ the change of the density of states associated with the CDW formation was estimated to be 0.1 states/eV atom per spin, corresponding to a bare Sommerfeld constant $\gamma = 9.2 \times 10^{-3}$ J/mol K. It thus gives a ratio of $\gamma^*/\gamma = 8.4$, about six times larger than the BCS value 1.43 within the weak-coupling limit, indicating the strong-coupling nature of this transition. Such enhancements in the specific-heat jumps from their mean-field values have been also reported in other CDW systems, such as a factor of 5 for 2H-TaSe₂ (Ref. 17) and a factor of 3 for K_{0.3}MoO₈ (Ref. 18).

The specific-heat anomaly can be related to the thermal expansion in accordance with the Ehrenfest relation for a second-order transition,

$$\Delta \alpha = - \left(\frac{\Delta C_p}{T_o} \right) \left(\frac{dT_o}{dP} \right). \quad (6)$$

TABLE II. Fitting parameters of specific heat of $\text{Lu}_5\text{Ir}_4\text{Si}_{10}$ to a model of critical fluctuations in addition to mean-field contributions.

Background term			Mean-field term			Fluctuations contribution		
a_1 (J/mol K)	a_2 (K)	a_3	γ^* (J/mol K ²)	β	b^- (J/mol K)	α^-	b^+ (J/mol K)	α^+
306	115	1.46	7.7×10^{-2}	6.0	1.54×10^{-3}	1.8	4.8×10^{-4}	2

at T_o . Substituting experimental values $\Delta\alpha = 4 \times 10^{-6} \text{ K}^{-1}$, $dT_o/dP = -1.4 \times 10^{-3} \text{ K/bar}$, and the mass density $\rho = 5.04 \times 10^3 \text{ mol/m}^3$ to the relation,^{1,4} it yields $\Delta C_p = 4.5 \text{ J/mol K}$, close to the estimated mean-field value 6.2 J/mol K but much smaller than the observed value $\Delta C_p = 55 \text{ J/mol K}$. In addition, taking the temperature region $\Delta T_G \sim 5 \text{ K}$ where the fluctuations are important, the coherence length ξ_0 of about 4.6 \AA can be extracted through the Ginzburg criteria $\Delta T_G = (T_o/32)(k_B/\pi\Delta C_p \xi_0^3)^2$. Such a short coherence length, indication of the strong interchain couplings in $\text{Lu}_5\text{Ir}_4\text{Si}_{10}$, is similar to other CDW materials of 4.4 \AA for $\text{K}_{0.3}\text{MoO}_3$ (Ref. 12) and 4.5 \AA for 2H-TaSe_2 (Ref. 14). The deduced short coherence length in $\text{Lu}_5\text{Ir}_4\text{Si}_{10}$ seems to meet the criteria of McMillan's model proposed for the strong-coupled CDW systems.¹¹ Accordingly, there is a large number of soft phonon modes in the transition region, which provide a substantial heat capacity arising from their occupation. This could explain the origin of the huge specific heat jump exhibited in $\text{Lu}_5\text{Ir}_4\text{Si}_{10}$.

B. Thermal conductivity

The representative thermal conductivity observed in the studied sample is shown in Fig. 3. At low temperatures, κ increases with temperature and a maximum appears around 40 K . This is a typical feature for the reduction of thermal scattering at lower temperatures.¹⁹ The maximum takes place at the temperature where the phonon mean free path is approximately equal to the crystal-site distance. After passing through the maximum, κ drops with increasing temperature, following an $1/T$ behavior. There is an abrupt jump associated with a well-defined peak in κ near the transition. Beyond the transition region, κ raises monotonically with temperature, tending to a linear variation.

Due to the metallic nature of this compound, the total thermal conductivity κ_T can be expressed as a sum of lattice, electronic, and anomalous terms,

$$\kappa_T = \kappa_p + \kappa_e + \Delta\kappa. \quad (7)$$

The lattice part κ_p is expected to follow $1/T$ behavior, while the electronic contribution κ_e can be determined by means of

the Wiedmann-Franz law: $\kappa_e \rho / T = L_o$. Here ρ is the dc electric resistivity and the Lorentz number $L_o = 2.45 \times 10^{-8} \text{ W } \Omega \text{ K}^2$. As plotted in Fig. 3 the lower line represents the calculated κ (combination of κ_p and κ_e), which matches very well to the experimental result, except for the anomalous peak and high-temperature deviation. (Note that the calculated results were vertically shifted down by 10 mW/cm K in Fig. 3 for clarity.) This analysis provides a clear confirmation that the abrupt drop in κ near T_o is essentially caused by the reduction of electronic contributions. After subtracting κ_p and κ_e the feature of anomalous part $\Delta\kappa$ can be obtained, as demonstrated in the insert of Fig. 3. An excess thermal conductivity $\Delta\kappa/\kappa$ was estimated to be approximately 15% at T_o ; to our best knowledge, this value represents the largest thermal-conductivity peak among CDW materials. While defects and inhomogeneities may wipe out the critical cusp in κ , our huge peaks in κ demonstrate that both have a minor effect in our samples. Apparently, the observation of this giant $\Delta\kappa$ cannot be simply explained by changes in electron-or phonon-scattering process at the transition. It is noted that the anomalies in thermal conductivity were also observed in $\text{K}_{0.3}\text{MoO}_3$ and $(\text{TaSe}_4)_2\text{I}$ at the CDW transitions, but with much broader peaks.¹⁸ Kwok and Brown associated the peak in κ (5%) with the specific-heat jump (6%) in the blue bronze as a result of heat carried by the soft phonon and mode occupation.¹⁸ Because the softening modes near $2k_F$ are propagating, the heat carried by the soft phonons is considerable and is responsible for the giant $\Delta\kappa$. Hence, both C_p and κ features around T_o could be qualitatively understood in terms of this picture.

Another peculiar feature of the measured data in thermal conductivity is its high-temperature variation. As one can see from Fig. 3, the high- T κ rises more rapidly than those expected from the electronic and phonon contributions. Such behavior has also been discovered in $\text{K}_{0.3}\text{MoO}_3$ and $(\text{TaSe}_4)_2\text{I}$ (Ref. 18), which was attributed to the quasiparticle scattering due to fluctuations, which gives a linear increase in κ at higher temperatures.²⁰ Consequently, a large number of soft Kohn-Peierls phonons would contribute to the high- T thermal conductivity.

 TABLE III. Representative values of critical exponents α^- and α^+ and their corresponding standard deviations for the fit.

Critical exponents	$\alpha^- = \alpha^+$ =0.5	$\alpha^- = \alpha^+$ =1.0	$\alpha^- = \alpha^+$ =1.5	$\alpha^- = \alpha^+$ =2.0	$\alpha^- = \alpha^+$ =2.5	Best fit $\alpha^- = -1.8$ $\alpha^+ = 2.0$	$b^- \ln t $ $b^+ \ln t $
Standard deviations	11.47	7.75	0.85	0.69	29.45	0.15	10.95

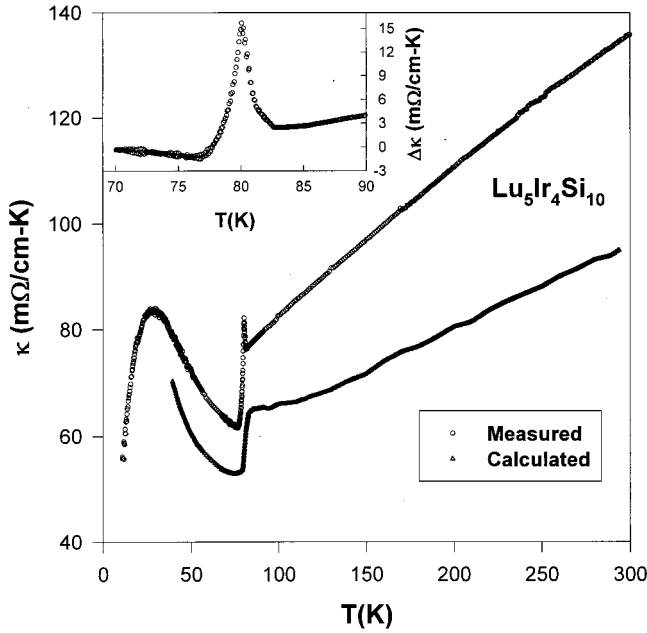


FIG. 3. Thermal conductivity vs temperature for $\text{Lu}_5\text{Ir}_4\text{Si}_{10}$. The lower curves represent the combination of lattice and electronic contributions to κ . Note that the calculated results have been vertically shifted down by 10 mW/cm K for clarity. Inset: excess thermal conductivity $\Delta\kappa$ in the vicinity of the CDW transition.

C. Thermoelectric power

Figure 4 displays the temperature-dependent thermoelectric power for $\text{Lu}_5\text{Ir}_4\text{Si}_{10}$. In the normal state, the data show quasilinear behavior with positive values, signifying that

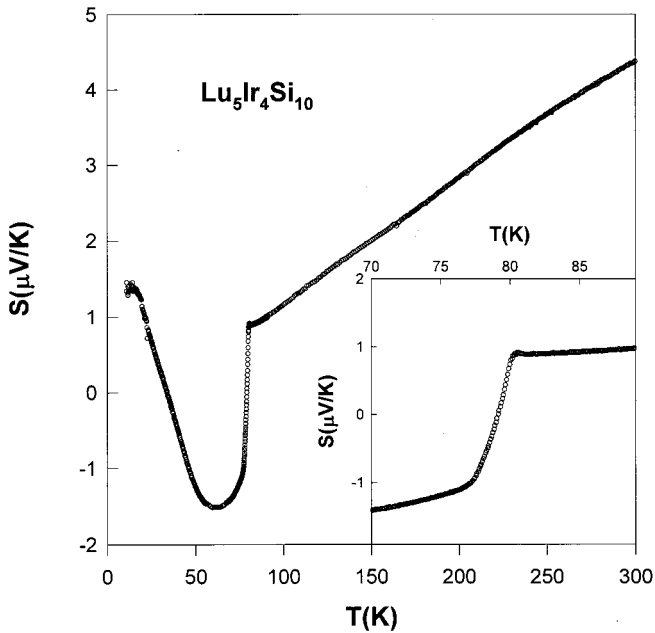


FIG. 4. Thermoelectric power as a function of temperature for $\text{Lu}_5\text{Ir}_4\text{Si}_{10}$. A rapid change of the sign in thermoelectric power in the vicinity of T_o is observed. The inset shows the details near the transition.

hole-type carriers dominate the high- T TEP. With decreasing temperature, the TEP changes sign from positive values above T_o to negative values below T_o , indicating a change of conduction mechanism or dominant carrier at this temperature. Upon further cooling the TEP increases again, ascribed to the phonon-drag effect, which is positive for the umklapp phonon-phonon scattering process.²¹ The rapid decrease from a positive to a negative thermoelectric power in the vicinity of T_o is attributed to the sudden change of the band structure associated with the electron-hole asymmetry. The fact that the Fermi-level density of states of $\text{Lu}_5\text{Ir}_4\text{Si}_{10}$ is sensitive to both external pressure² and internal pressure⁵ (impurity effects) is consistent with this scenario. Our present TEP study further indicates that $\text{Lu}_5\text{Ir}_4\text{Si}_{10}$ contains light hole pockets and heavy electron pockets in its energy band below the transition, but in the high-temperature regime the holes are heavier and thus dominate the TEP. This provides valuable information for future band-structure calculations on $\text{Lu}_5\text{Ir}_4\text{Si}_{10}$ and related compounds. Similar behavior has been found in other CDW systems, such as TiSe_2 and monophosphate tungsten bronzes $(\text{PO}_2)_4(\text{WO}_3)_{2m}$, and results were interpreted by the same argument.^{22,23}

It is known that the TEP measurement is a sensitive probe of energy relative to the Fermi surface and the results will yield information about the Fermi-level band structure. Since the high- T TEP varies linearly with temperature, one can try to extract the value of E_F through the classical formula $S = \pi^2 k_B^2 T / 2eE_F$, assuming a one-band model with an energy-independent relaxation time. The value of $E_F \sim 2.2$ eV was thus obtained by fitting the data between 100 and 300 K. Note that this value represents a lower limit, because other effects such as the CDW fluctuations could contribute to additional high- T TEP with a linear temperature variation. However, this estimate is in good agreement with the metallic nature of $\text{Lu}_5\text{Ir}_4\text{Si}_{10}$.

IV. CONCLUSIONS

In conclusion, thermal properties including specific heat, thermal conductivity, and thermoelectric power in $\text{Lu}_5\text{Ir}_4\text{Si}_{10}$ were studied in details. A huge ΔC_p ($\Delta C_p / C_p = 26\%$) with sharp specific-heat anomaly ($\Delta T_o / T_o = 1\%$) is found at T_o . This is quite unusual, as milder and broader transitions are normally seen in conventional CDW systems. No thermal hysteresis has been observed near T_o within the resolution limit of our apparatus, suggesting a possible second-order phase transition. Moreover, the specific-heat data were analyzed quantitatively in the framework of the critical fluctuation model near its CDW transition temperature. The critical exponent $\alpha \sim 2$ obtained from the best fit is much larger than the extended mean-field expectation of $\alpha = 0.5$ assuming 3D fluctuations. Also the ratio $\gamma^* / \gamma = 8.4$ for $\text{Lu}_5\text{Ir}_4\text{Si}_{10}$ is about six times-larger than the BCS value 1.43 of the weak-coupling limit, indicating the strong-coupling nature of this phase transition. An abrupt jump associated with a well-defined peak ($\Delta\kappa / \kappa = 15\%$) in κ is discovered near T_o . The calculated $\kappa (= \kappa_p + \kappa_e)$ matches very well with the measured data, indicating that the significant reduction in κ around T_o is mainly due to the deficiency of conduction elec-

trons. Although the peak in κ at T_o cannot be simply explained by changes in the electron-or phonon-scattering process, the observation of huge jumps in both specific heat and thermal conductivity at the phase transition are consistent with the consequence of heat carried by the soft phonon and mode occupation. In addition, the rapid change in the sign of thermoelectric power gives a better understanding of the evolution of electronic band structure of the system below and above the CDW formation. This provides valuable information for future band-structure calculations on $\text{Lu}_5\text{Ir}_4\text{Si}_{10}$ and its isostructural compounds.

Apparently, the observation of CDW transition in $\text{Lu}_5\text{Ir}_4\text{Si}_{10}$ is unique and cannot be fully understood by conventional CDW models. Thus more experimental and theo-

retical works are required to further verify whether this unusual CDW transition occurs only in the $\text{So}_5\text{Co}_4\text{Si}_{10}$ -type intermetallics, and whether it needs a new picture beyond the classical CDW model to interpret these anomalous thermal properties exhibited in $\text{Lu}_5\text{Ir}_4\text{Si}_{10}$.

ACKNOWLEDGMENTS

We are grateful to Professor J. W. Brill for the assistance of the DSC measurement and Professor R. N. Shelton for the early guidance of related projects. This work was supported by the National Science Council, Taiwan under Grant Nos. NSC-89-2112-M-259-018 (Y.K.K.) and NSC-89-2112-M-110-043 (H.D.Y.).

*Electronic address: yang@mail.phys.nsysu.edu.tw

- ¹R. N. Shelton, L. S. Hausermann-Berg, P. Klavins, H. D. Yang, M. S. Anderson, and C. A. Swenson, *Phys. Rev. B* **34**, 4590 (1986).
- ²H. D. Yang, R. N. Shelton, and H. F. Braun, *Phys. Rev. B* **33**, 5062 (1986).
- ³P. J. Chu, B. C. Gerstein, H. D. Yang, and R. N. Shelton, *Phys. Rev. B* **37**, 1796 (1988).
- ⁴C. A. Swenson, R. N. Shelton, P. Klavins, and H. D. Yang, *Phys. Rev. B* **43**, 7668 (1991).
- ⁵H. D. Yang, P. Klavins, and R. N. Shelton, *Phys. Rev. B* **43**, 7681 (1991); **43**, 7676 (1991).
- ⁶L. Alcacer, *The Physics and Chemistry of Low Dimensional Solids* (Reidel, Boston, 1980).
- ⁷R. M. Fleming, F. J. DiSalvo, R. J. Cava, and J. V. Waszczak, *Phys. Rev. B* **24**, 2850 (1981).
- ⁸B. Becker, N. G. Patil, S. Ramakrishnan, A. A. Menovsky, G. J. Nieuwenhuys, J. A. Mydosh, M. Kohgi, and K. Iwasa, *Phys. Rev. B* **59**, 7266 (1999).
- ⁹F. Galli, S. Ramakrishnan, T. Taniguchi, G. J. Nieuwenhuys, J. A. Mydosh, S. Geupel, J. Ludecke, and S. Van Smaalen, *Phys. Rev. Lett.* **85**, 158 (2000).
- ¹⁰N. P. Ong and P. Monceau, *Phys. Rev. B* **16**, 3443 (1977); N. P. Ong and J. W. Brill, *ibid.* **18**, 5265 (1978).
- ¹¹W. L. McMillan, *Phys. Rev. B* **16**, 643 (1977).
- ¹²R. F. Sullivan and G. Seidel, *Phys. Rev.* **173**, 679 (1968); M. B. Salamon, *Phys. Rev. B* **2**, 214 (1970).
- ¹³Y. Wang, M. Chung, T. N. O'Neal, and J. W. Brill, *Synth. Met.* **46**, 307 (1992).
- ¹⁴R. A. Craven and S. F. Meyer, *Phys. Rev. B* **16**, 4583 (1977).
- ¹⁵J. W. Brill, M. Chung, Y.-K. Kuo, X. Zhan, and E. Figueroa, *Phys. Rev. Lett.* **74**, 1182 (1995).
- ¹⁶M. Chung, Y.-K. Kuo, X. Zhang, E. Figueroa, J. W. Brill, and G. Mozurkewich, *Synth. Met.* **71**, 1891 (1995).
- ¹⁷R. S. Kwok, G. Gruner, and S. E. Brown, *Phys. Rev. Lett.* **65**, 365 (1990).
- ¹⁸R. S. Kwok and S. E. Brown, *Phys. Rev. Lett.* **63**, 895 (1989).
- ¹⁹R. Berman, *Thermal Conduction in Solids* (Clarendon, Oxford, 1976).
- ²⁰Kazumi Maki, *Phys. Rev. B* **46**, 7219 (1992).
- ²¹F. J. Blatt, P. A. Schroeder, C. L. Foiles, and D. Greig, *Thermoelectric Power of Metals* (Plenum, New York, 1976).
- ²²J. H. Gaby, B. DeLong, F. C. Brown, R. Kirby, and F. Levy, *Solid State Commun.* **39**, 1167 (1981).
- ²³C. Hess, C. Schlenker, J. Dumas, M. Greenblatt, and Z. S. Teweldemedhin, *Phys. Rev. B* **54**, 4581 (1996).